controls also in the harsh *in vivo* conditions (Figure 8B). Furthermore, this data suggests that the myoblast sheets remain at the location of transplantation after surgery.

DISCUSSION

In AMI, the occlusion of a coronary artery blocks the oxygen and nutrient supply to the myocardium it supplied, and causes severe stress as well as cell death (16). Under these conditions, cell death occurs via several mechanisms ranging from programmed apoptosis to overt necrosis (27). The dying cells release mediators that not only alert the immune system, but also promote cell death and exacerbate the damage (32). Moreover, reperfusion may further aggravate the rate of cell death (28). Prior studies have shown that Bcl-2 expression can protect cells transplanted for therapy by injection under these conditions (19). In this study, we investigated the ability of anti-apoptotic Bcl-2 in myoblasts to functionally enhance cell sheet transplantation in a rat model of AMI. We show here that Bcl-2 expression can enhance the novel technique of myoblast sheet transplantation. Sheets expressing Bcl-2 had increased tolerance for apoptotic stimuli, and survived longer when transplanted on top of infarcted myocardium. Moreover, we show that introducing Bcl-2 expression in myoblast sheets lead to their enhanced production of proangiogenic mediators, specifically VEGF and PlGF. Therapy with Bcl-2-expressing myoblast sheets significantly improved cardiac function, reduced fibrosis, enhanced myocardial neoangiogenesis and cell proliferation, and increased the amount of the stem cell antigen, c-kit, positive cells in the myocardium.

Bcl-2 localizes intracellularly to mitochondrial, nuclear, and endoplasmic reticulum membranes (1). It protects cells from death stimuli, such as nutrient deprivation (36), by stabilizing the mitochondrial membrane potential (30), reducing caspase activation, or inhibiting cytochrome c release (9). While tissue regeneration therapies and cell transplantation therapy aim to replace dead cells with progenitors as well as introducing growth-promoting signals to the tissue environment (19), it is frequently forgotten that transplanted cells face the same severe surroundings.

Although studies have demonstrated the superiority of cell sheet therapy to intra-myocardial injections in heart failure (20), transplantation of several sheets is required to counteract the struggle for survival, nutrients, and oxygen.

Mechanisms of cell death operating under ischemia and infarction depend on the location of cells in relation to the area supplied by the stenosed or occluded artery. Overt necrosis is predominant in the core areas, with programmed death by apoptosis gaining more ground towards the border areas with some collateral blood flow. The restricted oxygen and nutrient supply along with cell debris released by necrotic cells, elicits cell death responses that operate through common mechanisms, such as the generation of reactive oxygen species (16), and target mitochondrial function (26). In this study, we mimicked these *in vivo* conditions in cell culture by removing serum from the culture medium, thus depriving cells of nutrients and growth factors. Moreover, to reproduce the pro-apoptotic environment of the infarcted area, we treated cells with staurosporine, a widely used inducer of apoptosis that elicits similar intracellular apoptotic cascades that spur cell death in infarcted myocardium (10). Bcl-2 overexpression in cells and cell sheets provided protection and resistance against both nutrient deprivation and staurosporine-induced apoptosis. Importantly, when stressed with nutrient deprivation myoblast sheets expressing Bcl-2 differentiated into myotubes. This suggests that expression of antiapoptotic Bcl-2 does not prevent the myoblasts to exit the cell cycle, fuse, and differentiate.

These results show the benefit of *bcl-2* gene transduction for cell sheet transplantation, and corroborate with previous data on Bcl-2 expression inhibiting the mitochondrial pathway of apoptosis (18) activated by various stress factors including serum deprivation (2) and oxidative stress (7). Interestingly, previous studies have shown that Bcl-2 expression, when introduced in the heart, provides myocardial protection against ischemia (13), and further validates our approach. Thus, the introduction of *bcl-2* as a controlled pre-transplantation gene therapy can be considered beneficial for

promoting the effects of cell sheets under ischemic or infarcted tissues in prevailing pro-apoptotic or nutrient-deprived environments.

The finding that Bcl-2 expression only influences gene expression in cell sheets suggests that Bcl-2 does not alter cell behavior under normal growth conditions, Bcl-2 activity specifically enhances apoptosis tolerance, and that formation of cell sheets may induce apoptotic stress to the cells. These results show that when applying cell sheet therapy, prevention of apoptotic death already at the initial steps of sheet formation is necessary for maximizing therapeutic efficacy. In the Bcl-2-expressing myoblast sheets we observed enhanced production of the VEGF-family paracrine effectors, VEGF-A and PlGF. These growth factors are known to synergize in proangiogenic signaling (24), and further add to the beneficial profile induced by introduction of Bcl-2. In a previous study, Memon and colleagues reported that the myocardium under the myoblast sheets produces growth factors, such as VEGF (20). In this study, we show that wild type myoblast sheets themselves exhibit enhanced production of proangiogenic factors as compared to standard cultures of myoblasts, and that expression of Bcl-2 in sheets greatly enhances the production of these paracrine factors.

To further test the Bcl-2-mediated functional therapeutic benefit *in vivo* in AMI, wild type and Bcl-2-expressing sheets were transplanted onto the ischemic myocardium after LAD ligation. In the group undergoing Bcl-2 sheet transplantation, clearly enhanced left ventricular function was already evident at 10 days and was sustained until the end of the study period, 28 days after transplantation. LVEF paralleled LVFS as an alternate measure for left ventricular performance. Although some studies have reported enhanced cardiac function by unmodified myoblast sheets in experimental models of MI (11,20), treatment with two layers of wild type sheets in this study did not significantly increase LVEF. Here, however, transplantation of wild type sheets also counteracted the LVEF decline after MI. This may be due to

differences in rat strain (20), host species of donor myoblasts (11), the low number of cell sheets used, or the acute infarction model employed in the current study. Furthermore, due to generation and passage of the L6 cell line, differences to primary cells, as used in some studies, may emerge (35). Sheet transplantation increased vascular density in infarcted and border areas as evaluated by vWF immunostaining. Only the Bcl-2-modified sheet therapy increased both the number of proliferating cells in the remote area and the number of cells positive for stem cell antigen c-kit in the myocardium. In view of a recent report by Cimini et al. (8), these results suggest that more stem cells are stimulated to infiltrate the myocardium by Bcl-2-modified myoblast sheet therapy. Induction of stem cell infiltration can subsequently activate the endogenous repair processes of the myocardium (8). The observed effects on angiogenesis, proliferation, and c-kit expression were associated with an antifibrotic effect of the sheets at 28 days. Furthermore, overexpression of Bcl-2 resulted in prolonged survival of myoblast sheets *in vivo*, providing sustained secretion of angiogenic factors. The importance of such paracrine activators from myoblasts was demonstrated by Perez-Ilzarbe and colleagues on endothelial, smooth muscle, and cardiomyocyte cells (25). Activation of all these cell types is required for efficient repair of the damaged myocardium.

Taken together these results suggest that Bcl-2 overexpression in the myoblast sheets enhances their therapeutic potential by improving and sustaining the paracrine effects of the sheets in AMI. To our knowledge, this study presents the first combination therapy approach to use gene therapy-engineered cell sheets that can withstand apoptosis induction by means of Bcl-2 expression. These results provide the first insight on how anti-apoptotic and mitochondrioprotective strategies not only functionally but also by specific modification of gene expression profile can enhance the novel approach of cell sheet transplantation therapy in treatment of heart failure. Because myoblast sheet transplantation has shown no adverse effects in either preclinical or clinical

settings (Y. Sawa, personal communication), it seems feasible to adopt this cell transplantation methodology for gene modification and as vehicle in gene therapy as well. The transplantation of sheets can easily be carried out in conjunction with coronary artery bypass surgery, and it produces minimal damage to the heart muscle as compared to cell injections. The cells can be transduced with an optimized minimal amount of viral vector, and no viral vectors are injected to the patient. However, clinical trials are warranted to unambiguously demonstrate the efficacy of cell sheet transplantation.

ACKNOWLEDGEMENTS

This project was supported by Academy of Finland and the Japanese Society for the Promotion of Science. We thank Lahja Eurajoki for her help with the cell cultures and measurements, Irina Suomalainen for the immunohistochemical staining and Anne Reijula for the tissue processing. We also thank Veikko Huusko, Virpi Norppo, Kari Savelius, and Olli Valtanen for all their help and for the excellent animal care.

CONFLICTS OF INTEREST

The authors do not have any conflicts of interest.

REFERENCES

1. Adams, J. M.; Cory, S. The Bcl-2 protein family: arbiters of cell survival. Science 281:1322-1326; 1998.

2. Bialik, S.; Cryns, V. L.; Drincic, A.; Miyata, S.; Wollowick, A. L.; Srinivasan, A.; Kitsis, R. N. The mitochondrial apoptotic pathway is activated by serum and glucose deprivation in cardiac myocytes. Circ. Res. 85:403-414; 1999.

3. Bizik, J.; Kankuri, E.; Ristimaki, A.; Taieb, A.; Vapaatalo, H.; Lubitz, W.; Vaheri, A. Cell-cell contacts trigger programmed necrosis and induce cyclooxygenase-2 expression. Cell Death Differ. 11:183-195; 2004.

4. Bouju, S.; Lignon, M. F.; Pietu, G.; Le Cunff, M.; Leger, J. J.; Auffray, C.; Dechesne, C. A. Molecular cloning and functional expression of a novel human gene encoding two 41-43 kDa skeletal muscle internal membrane proteins. Biochem. J. 335:549-556; 1998.

5. Chao, D. T.; Korsmeyer, S. J. BCL-2 family: regulators of cell death. Annu. Rev. Immunol. 16:395-419; 1998.

6. Chinnaiyan, A. M.; Orth, K.; O'Rourke, K.; Duan, H.; Poirier, G. G.; Dixit, V. M. Molecular ordering of the cell death pathway. Bcl-2 and Bcl-xL function upstream of the CED-3-like apoptotic proteases. J. Biol. Chem. 271:4573-4576; 1996.

7. Choi, H.; Kim, S. H.; Chun, Y. S.; Cho, Y. S.; Park, J. W.; Kim, M. S. In vivo hyperoxic preconditioning prevents myocardial infarction by expressing bcl-2. Exp. Biol. Med. (Maywood). 231:463-472; 2006.

8. Cimini, M.; Fazel, S.; Zhuo, S.; Xaymardan, M.; Fujii, H.; Weisel, R. D.; Li, R. K. C-Kit Dysfunction Impairs Myocardial Healing After Infarction. Circulation 116:I77-82; 2007.

9. Crow, M. T.; Mani, K.; Nam, Y. J.; Kitsis, R. N. The mitochondrial death pathway and cardiac myocyte apoptosis. Circ. Res. 95:957-970; 2004.

10. Gil, J.; Almeida, S.; Oliveira, C. R.; Rego, A. C. Cytosolic and mitochondrial ROS in staurosporine-induced retinal cell apoptosis. Free Radic. Biol. Med. 35:1500-1514; 2003.

11. Hamdi, H.; Furuta, A.; Bellamy, V.; Bel, A.; Puymirat, E.; Peyrard, S.; Agbulut, O.; Menasche, P. Cell delivery: intramyocardial injections or epicardial deposition? A head-to-head comparison. Ann. Thorac. Surg. 87:1196-1203; 2009.

12. Hata, H.; Matsumiya, G.; Miyagawa, S.; Kondoh, H.; Kawaguchi, N.; Matsuura, N.; Shimizu, T.; Okano, T.; Matsuda, H.; Sawa, Y. Grafted skeletal myoblast sheets attenuate myocardial remodeling in pacing-induced canine heart failure model. J. Thorac. Cardiovasc. Surg. 132:918-924; 2006.

13. Imahashi, K.; Schneider, M. D.; Steenbergen, C.; Murphy, E. Transgenic expression of Bcl-2 modulates energy metabolism, prevents cytosolic acidification during ischemia, and reduces ischemia/reperfusion injury. Circ. Res. 95:734-741; 2004.

14. Klefstrom, J.; Vastrik, I.; Saksela, E.; Valle, J.; Eilers, M.; Alitalo, K. c-Myc induces cellular susceptibility to the cytotoxic action of TNF-alpha. EMBO J. 13:5442-5450; 1994.

15. Kondoh, H.; Sawa, Y.; Miyagawa, S.; Sakakida-Kitagawa, S.; Memon, I. A.; Kawaguchi, N.; Matsuura, N.; Shimizu, T.; Okano, T.; Matsuda, H. Longer preservation of cardiac performance by sheet-shaped myoblast implantation in dilated cardiomyopathic hamsters. Cardiovasc. Res. 69:466-475; 2006.

16. Krijnen, P. A.; Nijmeijer, R.; Meijer, C. J.; Visser, C. A.; Hack, C. E.; Niessen, H. W. Apoptosis in myocardial ischaemia and infarction. J. Clin. Pathol. 55:801-811; 2002.

17. Kutschka, I.; Kofidis, T.; Chen, I. Y.; von Degenfeld, G.; Zwierzchoniewska, M.; Hoyt, G.; Arai, T.; Lebl, D. R.; Hendry, S. L.; Sheikh, A. Y.; Cooke, D. T.; Connolly, A.; Blau, H. M.; Gambhir, S. S.; Robbins, R. C. Adenoviral human BCL-2 transgene expression attenuates early donor cell death after cardiomyoblast transplantation into ischemic rat hearts. Circulation 114:I174-180; 2006.

18. Kuwana, T.; Newmeyer, D. D. Bcl-2-family proteins and the role of mitochondria in apoptosis. Curr. Opin. Cell Biol. 15:691-699; 2003.

19. Li, W.; Ma, N.; Ong, L. L.; Nesselmann, C.; Klopsch, C.; Ladilov, Y.; Furlani, D.; Piechaczek, C.; Moebius, J. M.; Lutzow, K.; Lendlein, A.; Stamm, C.; Li, R. K.; Steinhoff, G. Bcl-2 engineered MSCs inhibited apoptosis and improved heart function. Stem Cells 25:2118-2127; 2007.

20. Memon, I. A.; Sawa, Y.; Fukushima, N.; Matsumiya, G.; Miyagawa, S.; Taketani, S.; Sakakida, S. K.; Kondoh, H.; Aleshin, A. N.; Shimizu, T.; Okano, T.; Matsuda, H. Repair of impaired myocardium by means of implantation of engineered autologous myoblast sheets. J. Thorac. Cardiovasc. Surg. 130:1333-1341; 2005.

21. Naro, F.; Sette, C.; Vicini, E.; De Arcangelis, V.; Grange, M.; Conti, M.; Lagarde, M.; Molinaro, M.; Adamo, S.; Nemoz, G. Involvement of type 4 cAMP-phosphodiesterase in the myogenic differentiation of L6 cells. Mol. Biol. Cell 10:4355-4367; 1999.

22. Okano, T.; Yamada, N.; Okuhara, M.; Sakai, H.; Sakurai, Y. Mechanism of cell detachment from temperature-modulated, hydrophilic-hydrophobic polymer surfaces. Biomaterials 16:297-303; 1995.

23. Palojoki, E.; Saraste, A.; Eriksson, A.; Pulkki, K.; Kallajoki, M.; Voipio-Pulkki, L. M.; Tikkanen, I. Cardiomyocyte apoptosis and ventricular remodeling after myocardial infarction in rats. Am. J. Physiol. Heart Circ. Physiol. 280:H2726-2731; 2001.

24. Payne, T. R.; Oshima, H.; Okada, M.; Momoi, N.; Tobita, K.; Keller, B. B.; Peng, H.; Huard, J. A relationship between vascular endothelial growth factor, angiogenesis, and cardiac repair after muscle stem cell transplantation into ischemic hearts. J. Am. Coll. Cardiol. 50:1677-1684; 2007.

25. Perez-Ilzarbe, M.; Agbulut, O.; Pelacho, B.; Ciorba, C.; San Jose-Eneriz, E.; Desnos, M.; Hagege, A. A.; Aranda, P.; Andreu, E. J.; Menasche, P.; Prosper, F. Characterization of the paracrine effects of human skeletal myoblasts transplanted in infarcted myocardium. Eur. J. Heart Fail. 10:1065-1072; 2008.

26. Regula, K. M.; Ens, K.; Kirshenbaum, L. A. Mitochondria-assisted cell suicide: a license to kill. J. Mol. Cell. Cardiol. 35:559-567; 2003.

27. Saraste, A.; Pulkki, K.; Kallajoki, M.; Henriksen, K.; Parvinen, M.; Voipio-Pulkki, L. M. Apoptosis in human acute myocardial infarction. Circulation 95:320-323; 1997.

28. Scarabelli, T. M.; Gottlieb, R. A. Functional and clinical repercussions of myocyte apoptosis in the multifaceted damage by ischemia/reperfusion injury: old and new concepts after 10 years of contributions. Cell Death Differ. 11 Suppl 2:S144-152; 2004.

29. Seidel, M.; Borczynska, A.; Rozwadowska, N.; Kurpisz, M. Cell-based therapy for heart failure: skeletal myoblasts. Cell Transplant. 18:695-707; 2009.

30. Shimizu, S.; Konishi, A.; Kodama, T.; Tsujimoto, Y. BH4 domain of antiapoptotic Bcl-2 family members closes voltage-dependent anion channel and inhibits apoptotic

mitochondrial changes and cell death. Proc. Natl. Acad. Sci. U. S. A. 97:3100-3105; 2000.

31. Shimizu, T.; Yamato, M.; Isoi, Y.; Akutsu, T.; Setomaru, T.; Abe, K.; Kikuchi, A.; Umezu, M.; Okano, T. Fabrication of pulsatile cardiac tissue grafts using a novel 3-dimensional cell sheet manipulation technique and temperature-responsive cell culture surfaces. Circ. Res. 90:e40; 2002.

32. Umansky, S. R.; Tomei, L. D. Apoptosis in the heart. Adv. Pharmacol. 41:383-407; 1997.

33. Vaananen, A. J.; Salmenpera, P.; Hukkanen, M.; Rauhala, P.; Kankuri, E. Cathepsin B is a differentiation-resistant target for nitroxyl (HNO) in THP-1 monocyte/macrophages. Free Radic. Biol. Med. 41:120-131; 2006.

34. Vento, A.; Hammainen, P.; Patila, T.; Kankuri, E.; Harjula, A. Somatic stem cell transplantation for the failing heart. Scand. J. Surg. 96:131-139; 2007.

35. Yaffe, D. Retention of differentiation potentialities during prolonged cultivation of myogenic cells. Proc. Natl. Acad. Sci. U. S. A. 61:477-483; 1968.

36. Zhu, W.; Cowie, A.; Wasfy, G. W.; Penn, L. Z.; Leber, B.; Andrews, D. W. Bcl-2 mutants with restricted subcellular location reveal spatially distinct pathways for apoptosis in different cell types. EMBO J. 15:4130-4141; 1996.

TABLES

Table 1. Genes upregulated in Bcl-2-overexpressing L6 myoblast sheets as compared to wildtype cell sheets.

Gene name	*Fold change up*	*Description*
1372602_at	13.16	genethonin
1371126_x_at	8.017	granzyme B
1367782_at	7.712	cytochrome c oxidase, subunit VIa, polypeptide 2
1370694_at	6.571	tribbles homolog 3 (Drosophila)
1370464_at	6.491	ATP-binding cassette, sub-family B (MDR/TAP), member 1A
1369043_at	5.989	potassium voltage-gated channel, shaker-related subfamily, member 4
1397300_at	5.957	transcribed locus
1394681_at	5.947	aldo-keto reductase family 1, member C-like 1
1379402_at	5.815	ATP-binding cassette, sub-family C (CFTR/MRP), member 4
1386185_at	5.524	tripartite motif-containing 7
1368918_at	5.513	placental growth factor
1369772_at	5.027	solute carrier family 6 (neurotransmitter transporter, glycine), member 9
1373282_at	5.017	similar to mitochondrial carrier protein MGC4399
1389066_at	4.691	regulator of calcineurin 2
1369343_at	4.653	glutamate receptor interacting protein 1
1373807_at	2.244	vegf-A

Table 2. Echocardiography data at 3, 10, and 28 days after LAD-ligation and transplantation

3 days

	N	AWTd	PWTd	Dd	AWTs	PWTs	Ds	FS	EF
Sham	5	1.28±0.08	1.28±0.10	8.02±0.24	1.82±0.12	1.88±0.12	6.00±0.21	0.252±0.013	0.580±0.022
Control	22	1.18±0.04	1.45±0.04	8.18±1.13	1.21±0.04 †††	2.11±0.07	7.02±0.11 †††	0.140±0.012 †††	0.357±0.024 †††
L6-WT	17	1.08±0.06	1.45±0.05	7.84±0.18 *	1.06±0.06 †††,*	1.99±0.09	6.91±0.14 †††	0.116±0.010 †††	0.306±0.022 †††
L6-Bcl2	21	1.06±0.05 †,*	1.39±0.05	8.35±0.13 ‡	1.08±0.04 †††,*	2.07±0.07	7.34±0.14 †††,*,‡	0.121±0.010 †††	0.314±0.023 †††

10 days

	N	AWTd	PWTd	Dd	AWTs	PWTs	Ds	FS	EF
Sham	5	1.38±0.04	1.46±0.10	7.74±0.30	1.86±0.09	1.98±0.06	6.02±0.20	0.221±0.015	0.525±0.029
Control	22	0.58±0.03 †††	1.51±0.06	9.58±0.16 †††	0.58±0.03 †††	2.12±0.07	8.50±0.17 †††	0.114±0.008 †††	0.300±0.019 †††
L6-WT	17	0.59±0.04 †††	1.37±0.05 *	9.28±0.18 †††	0.65±0.05 †††	2.12±0.08	8.19±0.18 †††	0.114±0.010 †††	0.322±0.021 †††
L6-Bcl2	21	0.61±0.03 †††	1.44±0.06	9.44±0.17 †††	0.60±0.03 †††	2.33±0.08 †,*,‡	8.08±0.15 †††,*	0.144±0.010 †††,*,‡	0.378±0.019 †††,**,‡

28 days

	N	AWTd	PWTd	Dd	AWTs	PWTs	Ds	FS	EF
Sham	5	1.42±0.04	1.62±0.12	7.70±0.35	1.74±0.10	2.18±0.16	5.94±0.43	0.233±0.027	0.542±0.045
Control	22	0.60±0.03 †††	1.53±0.05	10.46±0.17 †††	0.61±0.03 †††	2.16±0.09	9.38±0.22 †††	0.106±0.008 †††	0.280±0.020 †††
L6-WT	17	0.55±0.04 †††	1.55±0.07	10.11±0.14 †††	0.52±0.04 †††,*	2.20±0.07	9.04±0.14 †††	0.106±0.006 †††	0.285±0.014 †††
L6-Bcl2	21	0.63±0.03 †††,‡	1.75±0.07 *,‡	10.61±0.17 †††	0.64±0.03 †††,‡	2.48±0.09 *,‡	9.27±0.18 †††	0.127±0.008 †††,*,‡	0.331±0.019 †††,*,‡

Values represent mean ± SEM

† $p<0.05$, ††† $p<0.001$ as compared to sham-operated group, * $p<0.05$ as compared to control group, ‡ $p<0.05$ as compared to L6-WT group

LEGENDS TO TABLES AND FIGURES

Table 1. Genes upregulated in Bcl-2-overexpressing L6 myoblast sheets as compared to wild type cell sheets.

Table 2. Echocardiography data at 3, 10, and 28 days after LAD ligation and transplantation showing anterior and posterior wall thickness in diastolic (AWTd, PWTd) and systolic phases (AWTs, PWTs) and left ventricular diameter in diastolic (Dd) and systolic (Ds) phases. Units are presented in mm. Dd and Ds were used to calculate fraction shortening (LVFS) and ejection fraction (LVEF) percentage.

Figure 1. Expressional and functional characterization of Bcl-2 in L6 myoblasts. A) Expression of Bcl-2 protein in wild type (L6-WT) and Bcl-2-overexpressing (L6-Bcl2) myoblasts. B) Immunofluorescence (IF) detection of Bcl-2 in L6 myoblasts suggesting cytoplasmic and perinuclear localization. C) Mitochondrial activity as measured with MTT assay in L6-WT and L6-Bcl2 in myoblast cultures treated for 48 hours. D) Number of adherent L6-WT and L6-Bcl2 myoblasts in cultures treated for 48 hours. E) Quantification of early apoptosis as measured by FITC-labeled annexin V binding to cell surface-translocated phosphatidyl serine. C-E) Cultures deprived of serum (left panels), and cultures with apoptosis induced by staurosporine (80 ng/ml) (right panels).

Figure 2. Immunohistochemistry, differentiation, and VEGF expression of wild type (L6-WT) and Bcl-2-overexpressing (L6-Bcl2) myoblast sheets. A) Hematoxylin and eosin (H&E) stain, expression of Bcl-2 protein, cell proliferation as detected by the expression of proliferation-associated Ki67 antigen and the evaluation of apoptotic cells by immunodetection for active cleaved caspase-3. B) Activation of caspase-3 in L6-WT and L6-Bcl2 myoblast sheets after 24 hours in control, serum-deprived, and staurosporine-treated (10 ng/ml) sheets. C) Immunoblots of myogenic differentiation markers troponin T and myogenin from L6-WT and L6-Bcl2 sheets after differentiation in serum-free medium for 96 hours. Lower panels show phase contrast images demonstrating the formation of myotubes in

L6-Bcl2 sheets. Cell detachment and death prevail in L6-WT sheets. D) Amount of VEGF-A in culture medium of untreated, serum-deprived, and staurosporine-treated L6-WT and L6-Bcl2 sheets as determined with ELISA.

Figure 3. Echocardiography for A) left ventricle ejection fraction (EF), and B) left ventricle fraction shortening at the indicated time points after wild type (n=17, L6-WT), Bcl-2-overexpressing (n=20, L6-Bcl2) myoblast sheet therapy for acute myocardial infarction (AMI). Control rats (n=22) underwent AMI without sheet transplantation, and sham-operated rats (n=5) underwent left-sided thoracotomy to control the surgery-induced effect on systolic parameters. * $p<0.05$, ** $p<0.01$ as compared to the control group; † $p<0.05$, †† $p<0.01$ as compared to the L6-WT group.

Figure 4. A) Quantitative evaluation of vascular density using immunohistochemical staining for von Willebrand factor (vWF) expression in myocardial paraffin-embedded sections from sham-operated, wild type (L6-WT), Bcl-2 (L6-Bcl2), and control animals. *$p<0.05$, ** $p<0.01$ as compared to the control group; † $p<0.05$, †† $p<0.01$ as compared to the L6-WT group. B) Expression of vWF in uninfarcted, sham-operated myocardium. C) Representative figures showing vascular density with vWF staining (brown) in infarct (left panels), border (middle panels), and remote (right panels) areas of the left ventricle. Sections were counterstained with hematoxylin (blue).

Figure 5. A) Quantitative evaluation of fibrosis by Sirius Red staining of myocardial paraffin-embedded sections from sham-operated, wild type (L6-WT), Bcl-2 (L6-Bcl2), and control animals. * $p<0.05$, ** $p<0.01$ as compared to the control group; † $p<0.05$, †† $p<0.01$ as compared to the L6-WT group. B) Background staining in uninfarcted, sham-operated myocardium. C) Representative figures showing the amount of fibrosis (red) in infarct (left panels), border (middle panels), and remote (right panels) areas of the left ventricle.

Figure 6. A) Quantitative evaluation of proliferative cells as assessed with the expression of proliferation associated Ki67 nuclear antigen (dark brown). Figure shows mean ± SEM densitometry values from the immunohistochemistry of myocardial paraffin-embedded

sections of sham-operated, wild type (L6-WT), Bcl-2 (L6-Bcl2), and control animals. * $p<0.05$, ** $p<0.01$ as compared to the control group, † $p<0.05$, †† $p<0.01$ as compared to the L6-WT group. B) Expression of Ki67 in uninfarcted, sham-operated myocardium. C) Representative figures of showing proliferating cells by Ki67 expression in infarct (left panels), border (middle panels), and remote (right panels) areas of the left ventricle. Sections were double-stained to detect muscle tissue by tropomyosin (red) expression. Sections were counterstained with hematoxylin (blue).

Figure 7. A) Quantitative evaluation of the number of c-kit expressing cells in the myocardium. Paraffin-embedded sections were stained from sham-operated, wild type (L6-WT), Bcl-2 (L6-Bcl2), and control animals. * $p<0.05$, as compared to the L6-WT group, ** $p<0.01$ as compared to the control group. B) Representative figures of c-kit expressing cells in the myocardium from sham-operated (upper left panel), control (upper right panel), L6-WT (lower left panel) and L6-Bcl2 (lower right panel) groups. Sections were counterstained with Nuclear Fast Red.

Figure 8. Quantitative evaluation of cell survival after myoblast cell sheet transplantation. A) Analysis of green fluorescence intensity from the apical surface of hearts 3 weeks after transplantation of GFP-expressing wild type (L6-WT-GFP, n=6) and Bcl-2-overexpressing (L6-Bcl2-GFP, n=6) cell sheets. B) Representative bright field (left panels) or fluorescence (right panels) images of excised hearts three weeks after surgery.

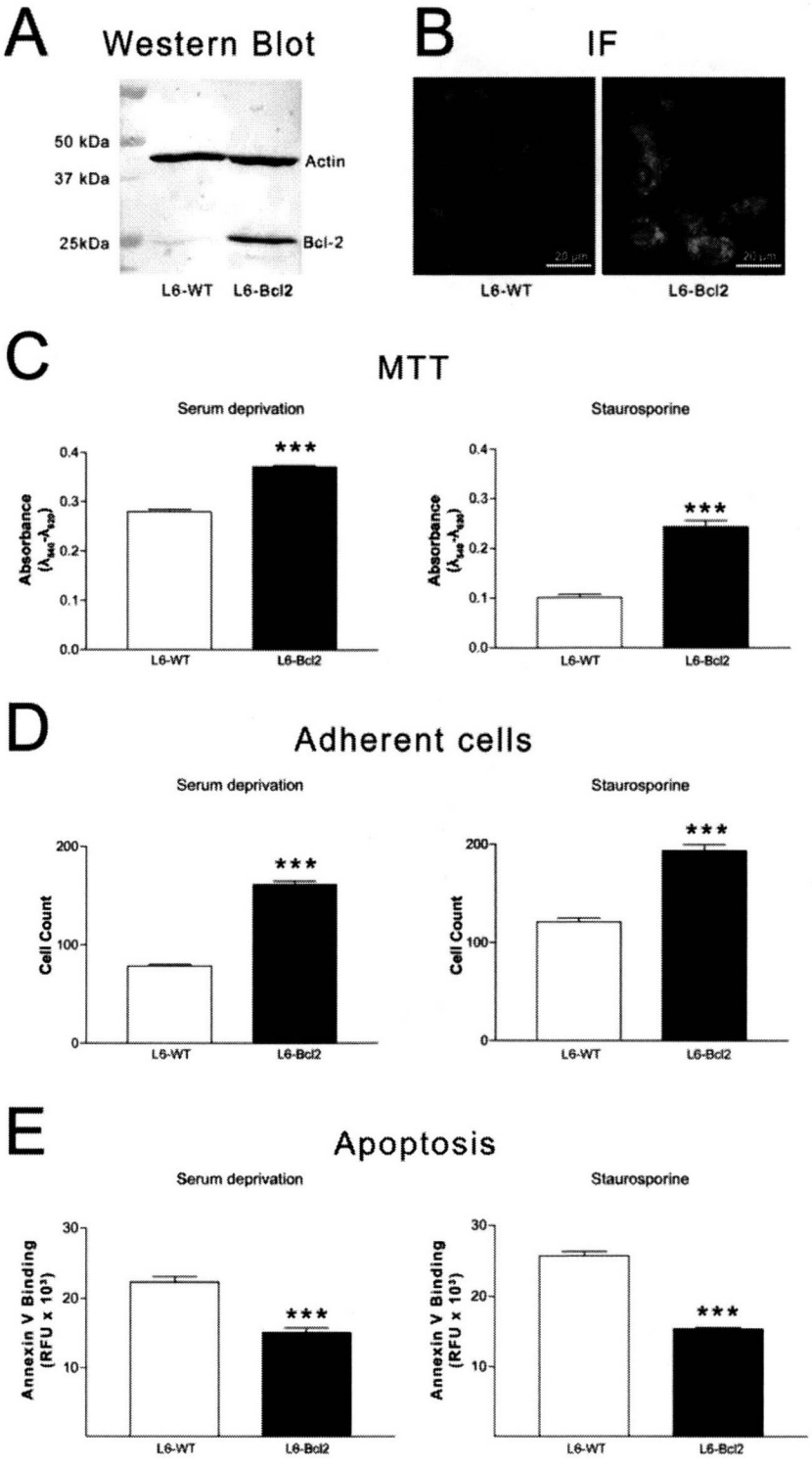
A
Western Blot
50 kDa
37 kDa
25kDa
Actin
Bcl-2
L6-WT
L6-Bcl2
B
IF
L6-WT
L6-Bcl2
C
MTT
Serum deprivation
Staurosporine
Absorbance
0.4
0.3
0.2
0.1
0.0
***
L6-WT
L6-Bcl2
D
Adherent cells
Serum deprivation
Staurosporine
Cell Count
200
100
0
***
L6-WT
L6-Bcl2
E
Apoptosis
Serum deprivation
Staurosporine
Annexin V Binding
(RFU x 10³)
30
20
10
***
L6-WT
L6-Bcl2

Figure 1:

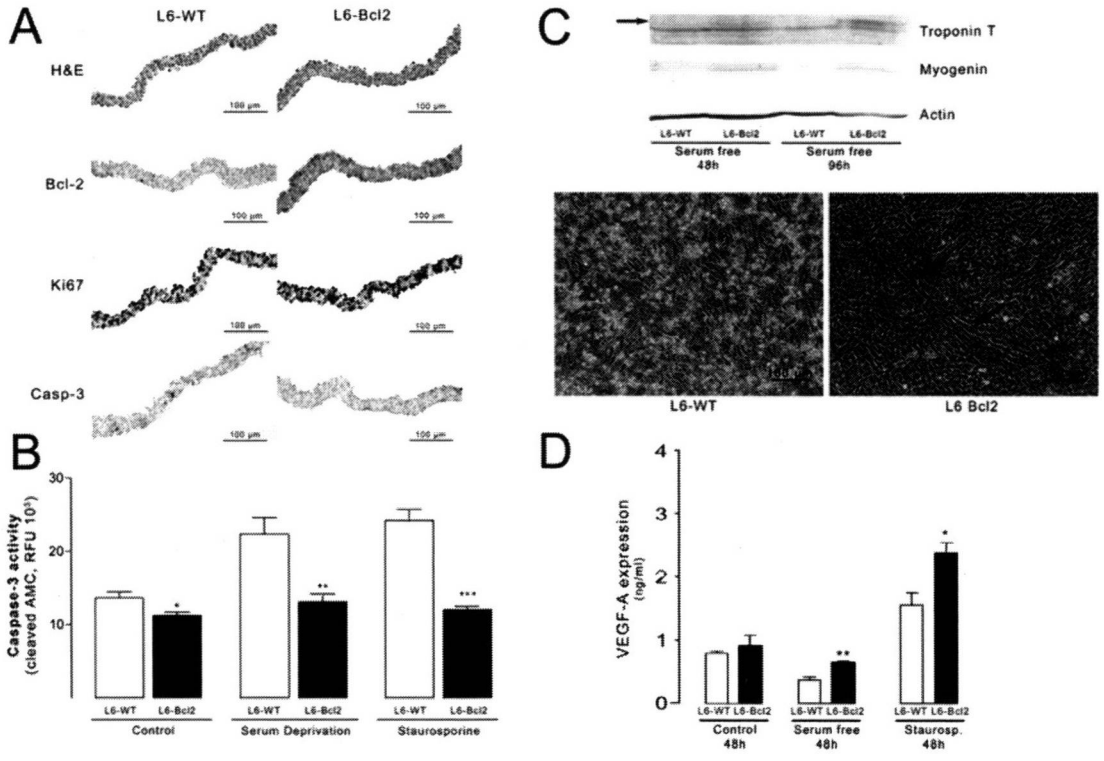
A
L6-WT
L6-Bcl2
H&E
Bcl-2
Ki67
Casp-3
100 µm
B
Caspase-3 activity
(cleaved AMC, RFU 10³)
30
20
10
*
**
***
L6-WT
L6-Bcl2
Control
Serum Deprivation
Staurosporine
C
Troponin T
Myogenin
Actin
L6-WT
L6-Bcl2
Serum free
48h
Serum free
96h
L6-WT
L6 Bcl2
D
VEGF-A expression
(ng/ml)
4
3
2
1
0
*
**
L6-WT L6-Bcl2
Control
48h
Serum free
48h
Staurosp.
48h

Figure 2:

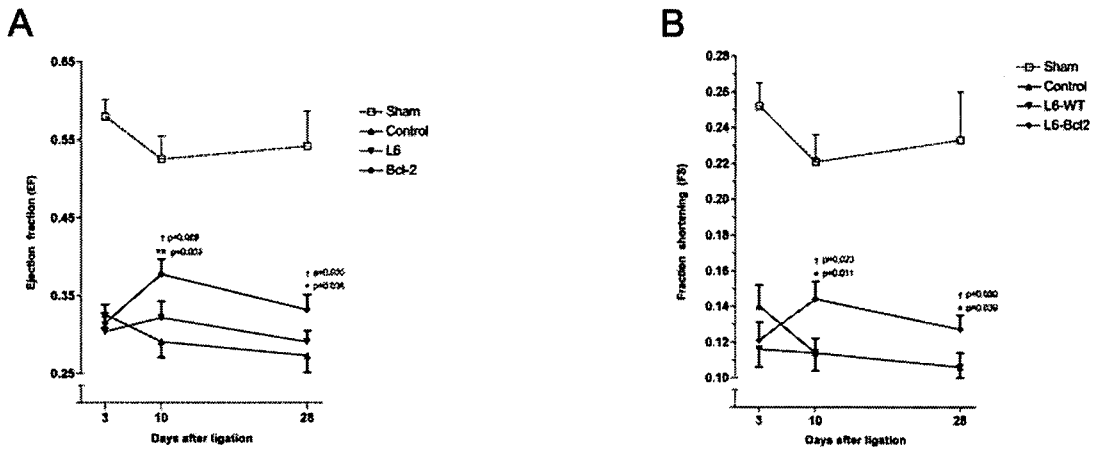
A
B
Sham
Control
L6
Bcl-2
L6-WT
L6-Bcl2
Ejection fraction (EF)
Fraction shortening (FS)
Days after ligation
3
10
28

Figure 3: